Quantum Electronics **49** (4) 330–336 (2019)

https://doi.org/10.1070/QEL16993

Generation of ultrashort X-ray bursts without attosecond frequency modulation in Coulomb collisions of nuclei of diatomic heteronuclear molecules ionised by an ultraintense laser pulse

I.R. Khairulin, M.Yu. Emelin, M.Yu. Ryabikin

Abstract. **Based on classical and quantum mechanical calculations, we study the possibility of generating ultrashort X-ray bursts, free of attosecond frequency modulation (attochirp), with photon energies of the order of 1 keV and higher in Coulomb collisions of nuclei in an ensemble of diatomic molecules containing nuclei with different masses, driven by ultraintense IR laser pulses. The minimally attainable duration of the generated X-ray pulses is investigated as a function of intensity and wavelength of laser radiation. It is shown that the considered mechanism of nuclear collisions makes it possible to generate transform-limited X-ray pulses with a duration of about 1 as using modern petawatt laser systems.**

Keywords: *molecules, femtosecond laser radiation, ionisation, nuclear collisions, attosecond pulses.*

1. Introduction

Recently, great progress has been made in the development of attosecond physics, an interdisciplinary field of research aimed at obtaining and measuring the characteristics of attosecond light pulses and at employing these pulses to probe and control ultrafast processes caused by electron dynamics in atoms, molecules, and condensed media [1–4]. The traditionally applied approach to obtaining attosecond pulses is based on the generation of high laser radiation harmonics [5–7]. Among the various schemes proposed to date, the generation of the shortest and most intense attosecond pulses is provided by a scheme using high harmonic generation (HHG) with tunnelling ionisation of gases [8, 9]. According to the semiclassical model [10, 11], the elementary act underlying HHG in gases is a three-step process in which an electron separates from an atom or molecule under the action of an alternating intense laser field, is accelerated by it and returns to the parent ion. As a result of a collision with the parent ion, a high-energy photon can be emitted. One of the most important achievements in the research related to HHG was the experimentally demonstrated generation of harmonics with photon energies exceeding 1 keV and high brightness [12]. Despite the fact that the experimentally obtained width of the harmonic spectrum, which is a fraction of a kiloelectronvolt, can ensure the generation of pulses with a duration of several attoseconds, the shortest high-harmonic radiation pulses obtained to date have a duration of 40–60 as [13–15]. An important factor limiting the duration of high-harmonic radiation pulses is the well-known property of the above-described three-stage HHG mechanism, which consists in the presence of frequency modulation of the harmonic signal within the laser field period, called attochirp [16, 17]. Attochirp, in terms of the classical electron trajectories in a laser field, arises due to the fact that electrons accelerated to different energies collide with the parent ion at different points in time.

To compensate for attochirp, various dispersive elements are used, such as thin metal films [18, 19], multilayer chirped X-ray mirrors [20] or gaseous media [21, 22]. However, these approaches have a number of limitations caused by the material properties, such as losses or finite width of the spectral range in which the dispersion behaves as desired. Other proposed schemes are based on the use of multicolour and/or chirped laser pulses to control the trajectories of free electrons [23, 24]. While these schemes can have great flexibility, their implementation in macroscopic volumes of nonlinear media is hampered by dispersion, causing phase mismatch and deviation of the waveforms of the interacting fields from optimal ones during their propagation.

Another approach to obtaining light pulses without attochirp involves the use of ionisation regimes other than tunnelling, namely, ionisation with suppression of the Coulomb barrier [25] or high-frequency stabilisation [26]. In these regimes, highly localised electron wave packets are formed, the collisions of which with an ion lead to the appearance of ultrashort bursts of radiation. The radiation resulting from these collisions, in essence, does not possess attochirp and therefore does not require special measures to compensate for it. We consider a process of a similar type, namely, the collision of nuclei in a diatomic heteronuclear molecule exposed to an ultraintense laser field. Processes of this type have been previously studied, for example, in [27–29]. While the generation of subattosecond bursts of radiation during such collisions was noted in [27] as an interesting side effect, the main attention in the above-mentioned studies was focused on the problem of laser fusion. In this paper, laser-induced Coulomb collisions of nuclei are investigated in detail as a source of extremely short high-frequency radiation pulses without attochirp.

I.R. Khairulin, M.Yu. Emelin, M.Yu. Ryabikin Institute of Applied Physics, Russian Academy of Sciences, ul. Ulyanova 46, 603950 Nizhny Novgorod, Russia; e-mail: mike@ufp.appl.sci-nnov.ru

Received 6 March 2019
Kvantovaya Elektronika **49** (4) 330–336 (2019)
Translated by I.A. Ulitkin

2. Classic model

Consider a molecule consisting of two nuclei: with mass M and charge Q and with mass m and charge q. We assume that the first nucleus is heavier than the second one, i.e. $M > m$. It is agreed that the molecule is affected by a uniform, ultraintense linearly polarised laser field with an amplitude rapidly increasing to values that are many orders of magnitude larger than that of the Coulomb field holding electrons near the nuclei. The time dependence of the electric field at the pulse front can be represented as $\boldsymbol{E} = E_0\exp(\gamma t)\sin(\Omega t)\boldsymbol{x}_0$, where γ is the increment of the rise of the laser field, Ω is its frequency, and $\boldsymbol{x}_0$ is the unit vector. Under the conditions described above, it can be approximately assumed that at $t = 0$ the molecule subjected to the laser field is already deprived of electrons, while the nuclei remain in their original position (characterised by an equilibrium inter-nuclear distance a_0 in a neutral molecule). The mutual positions of the nuclei are shown in Fig. 1.

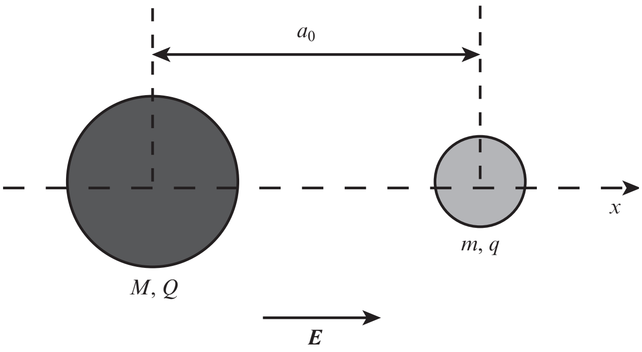

Figure 1. Positions of the nuclei in a diatomic heteronuclear molecule and its orientation relative to the electric field of the laser pulse at the initial moment of time.

In the centre of mass system, the two-particle problem in question is reduced to the problem of a single charged particle with an effective mass $\mu = mM/(m + M)$ and an effective charge $q_{\text{eff}} = \mu(q/m - Q/M)$ [30], which is affected by the Coulomb repulsive centre and the external electric field. Below, for simplicity, we limit our analysis to the one-dimensional case. The equation of motion of a particle in this case has the form

$$\mu\ddot{x} = \frac{qQ}{|x|^3}x + q_{\text{eff}}E_0\exp(\gamma t)\sin(\Omega t), \quad (1)$$

where x is the inter-nuclear distance. At the initial moment of time, the nuclei can be considered to be at rest. Therefore, as the initial conditions, we choose the conditions $x(t = 0) = a_0$ and $\dot{x}(t = 0) = 0$. Then, the solution of equation (1) has the form

$$x = \tilde{x} + x_1, \quad (2)$$

where x_1 is a particular solution of the equation

$$\mu\ddot{x} = q_{\text{eff}}E_0\exp(\gamma t)\sin(\Omega t), \quad (3)$$

and $\tilde{x}$ satisfies the equation

$$\ddot{\tilde{x}} = \frac{qQ/\mu}{|\tilde{x} + x_1(t)|^3}[\tilde{x} + x_1(t)] \quad (4)$$

with initial conditions

$$\tilde{x}(t = 0) = a_0 - x_1(t = 0), \quad \dot{\tilde{x}}(t = 0) = -\dot{x}_1(t = 0). \quad (5)$$

It is easy to show that the contribution of $\tilde{x}(t)$ to the total solution will decrease with increasing amplitude E_0 and wavelength Λ of the laser field in proportion to $(E_0\Lambda^2)^{-2}$. Therefore, in calculations of the classical particle trajectory, it can be neglected. This means that in the considered approximation, the nuclei do not interact with each other at the initial moment of time. Then, taking into account the initial conditions for the nuclear coordinates and velocities, the solution for $x(t)$ can be written as

$$x(t) = a_0 + \frac{2\alpha b}{(1+\alpha^2)^2} + \frac{b}{1+\alpha^2}\Omega t + \frac{b}{(1+\alpha^2)^2} \times[(\alpha^2 - 1)\exp(\alpha\Omega t)\sin(\Omega t) - 2\alpha\exp(\alpha\Omega t)\cos(\Omega t)], \quad (6)$$

where $\alpha = \gamma/\Omega$; the quantity $b = q_{\text{eff}}E_0/(\mu\Omega^2)$ at $\alpha = 0$ determines the amplitude of oscillations of an effective particle in an external electric field.

Solution (6) can be used to estimate the maximum photon energy that can be emitted in the collision of two nuclei. This energy coincides with the kinetic energy of the collision of nuclei, determined by the expression

$$\mathcal{E}_{\text{coll}} = \mu\dot{x}_1^2(t = t_{\text{coll}})/2, \quad (7)$$

where t_{coll} is the time of the first collision. One can see from Fig. 2 that the collision of nuclei occurs at the beginning of the second period of the field, and therefore it is possible to assume with good accuracy that $t_{\text{coll}} \approx T = \Lambda/c$. Then, differentiating (6) and substituting the resulting expression in (7), for the collision energy we obtain the expression:

$$\mathcal{E}_{\text{coll}} \approx \frac{\mu b^2\Omega^2}{2}\left[\frac{1 - \exp(2\pi\alpha)}{1+\alpha^2}\right]^2. \quad (8)$$

Thus, the collision energy is proportional to the product of the laser field intensity I_0 and the square of the wavelength: $\mathcal{E}_{\text{coll}} \propto I_0\Lambda^2$.

Below, as a computational example, we consider in more detail a neutral HD molecule, for which $m = m_{\text{p}}$, $M = 2m_{\text{p}}$, $q = Q = e$, where m_{p} is the proton mass. The initial distance

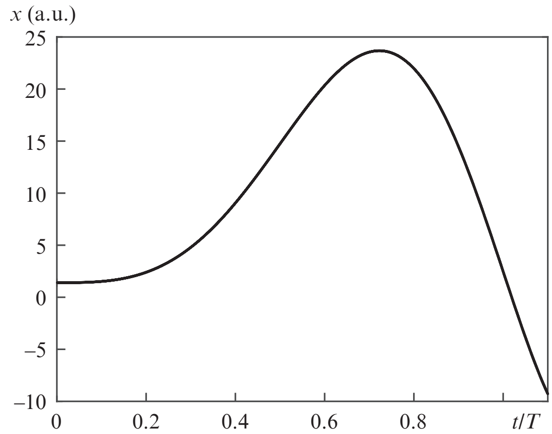

Figure 2. Classically calculated time dependence of the distance between the H and D nuclei when the HD molecule is subjected to the action of a laser field with intensity $I_0 = 3.3\times10^{19}$ W cm^{-2} and wavelength $\Lambda = 800$ nm.

between the nuclei is assumed to be equal to the value corresponding to the minimum of the potential function of the ground electron state of the HD molecule [31]: $a_0 \approx 1.401$ atomic units (a.u.). In addition, we assume the increment of the field increase γ to be such that the instantaneous field intensities in the neighbouring peaks differ 10 times: $\gamma = [\Omega/(2\pi)]\ln 10$.

Figure 3 shows the dependence of the nuclear collision energy [and, therefore, the maximum photon energy, which, according to formula (7), can be achieved in the collision of the nuclei of the molecular system in question] on the wavelength and laser radiation intensity. One can see that the estimate given by expression (8) describes with a good accuracy the dependence of the nuclear collision energy on the main parameters of the laser field. In the considered region of parameters, this energy can exceed 10 MeV; it should, however, be expected that only a small fraction of this energy will be converted into radiation. At $I_0 = 3.3\times10^{19}$ W cm^{-2} and $\Lambda = 2\pi c/\Omega = 800$ nm, the kinetic energy of the collision is $\mathcal{E}_{\rm coll} \approx 22.8$ keV.

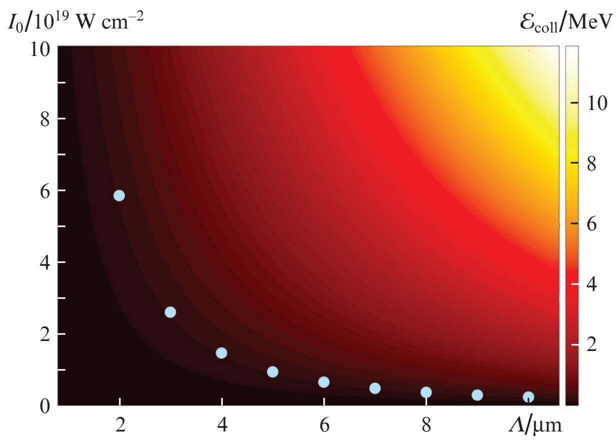

Figure 3. Dependence of the nucleus collision energy $\mathcal{E}_{\rm coll}$ (7) on the wavelength Λ and laser field intensity I_0. Light points correspond to an energy $\mathcal{E}_{\rm coll}$ = 25 keV, calculated by formula (8).

To assess the efficiency of photon generation, we can calculate the molecular dipole acceleration

$$\ddot{d}(t) = q_{\rm eff}\ddot{x}(t). \tag{9}$$

In the classical case, the second factor on the right-hand side of (9) can be found from expression (1), in which instead of $x(t)$ we should use the obtained solution (6) for the trajectory, and the interaction of the repulsive centre with the effective point particle should be replaced by the interaction with the nuclear cloud whose charge density is $q_{\rm eff}|\psi(x,t=0)|^2$, where $\psi(x,t=0)$ is the wave function of the ground state of the HD molecule at the initial moment of time. This wave function (Fig. 4) can be found by solving the stationary Schrödinger equation with a potential [31]. It should be noted that, since the wave function of the ground state of the molecule in the one-dimensional problem is symmetric about the position of the Coulomb centre, it is necessary to set $a_0 = 0$ in (6). The dipole acceleration can be divided into parts with linear and nonlinear dependences on the field. It is the nonlinear part that is responsible for the emergence of new frequency components in the spectrum; therefore, we will further consider

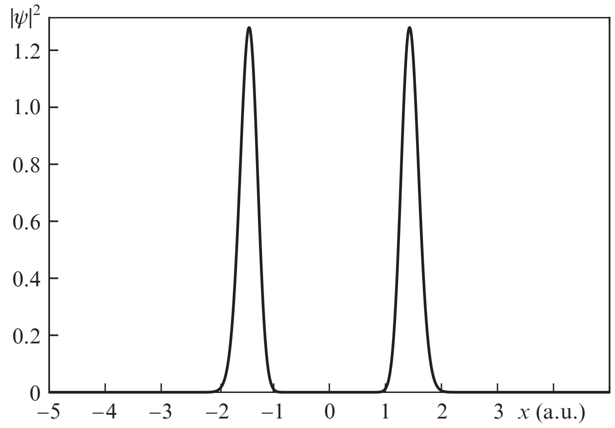

Figure 4. Probability density distribution along the nuclear coordinate for a neutral HD molecule in the ground state.

only this part of the dipole acceleration, which we call the polarisation response of the system. In view of the above, expression (9) can be rewritten as

$$\ddot{d}(t) = \frac{q_{\rm eff}qQ}{\mu}\int_{-\infty}^{\infty}\frac{x-x_1(t)}{|x-x_1(t)|^3}|\psi(x,t=0)|^2{\rm d}x. \tag{10}$$

Consider expression (10) in more detail. According to (10), the polarisation response is proportional to the overlap integral of the probability density distribution with a function describing the Coulomb interaction. Note that in the approximation used, we neglect the spreading of the nuclear wave packet, assuming that it does not change in any way when moving in an external laser field and, moreover, when colliding with a Coulomb centre. Thus, a two-humped nuclear distribution corresponding to the one-dimensional case (Fig. 4) moves as a whole along the trajectory defined by expression (6) (see Fig. 2). As a result, two polarisation bursts (Fig. 5) are formed near the moment of collision. Obviously, the left and right sides of the wave packet in Fig.4 correspond respectively to the formation of the first and second bursts. It should, however, be noted that the shape of the first burst in Fig. 5 should in fact be different. This is due to the fact that the left

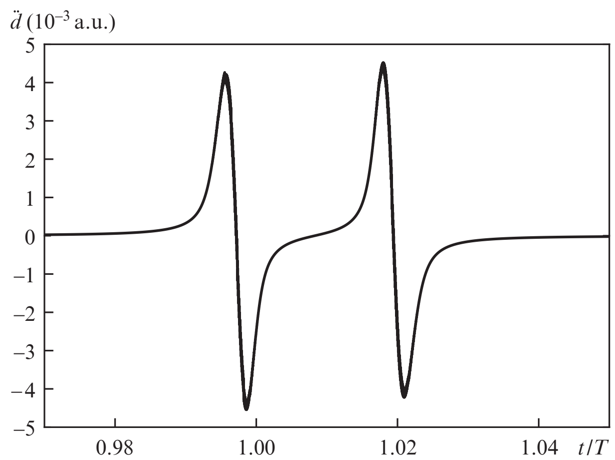

Figure 5. Classically calculated time dependence of the dipole acceleration $\ddot{d}$ near the moment of collision at the laser radiation intensity and wavelength of $I_0 = 3.3\times10^{19}$ W cm^{-2} and $\Lambda = 800$ nm.

side of the nuclear wave packet experiences a collision at a low energy $\mathcal{E}_{\rm coll}$ with the Coulomb centre already at the beginning of the first field period. The result of this should be a significant distortion of the shape of the left side of the wave packet and, therefore, a change in the properties (in particular, stretching) of the first burst in Fig. 5. In addition, in a model with a higher dimension, a collision at the beginning of the first field period should lead to a significant transverse delocalisation of the left side of the nuclear wave packet due to Coulomb repulsion, and it should be expected that the amplitude of the first burst formed during the collision in question will be much less than the amplitudes of the second burst.

This is confirmed by the results of two-dimensional quantum-mechanical numerical calculations shown in Fig. 6 (for details of these calculations, see Section 3). The calculations were performed for the same parameters of the laser field as those for Fig. 5. In the two-dimensional case, the probability density distribution over the nuclear coordinate at the initial moment of time has a ring-shaped structure with an average ring radius close to the equilibrium distance between the nuclei in the HD molecule. Under the action of a linearly polarised laser field that increases in amplitude, this ring-shaped distribution oscillates with an increasing amplitude along the polarisation direction of the electric field and at a sufficiently high field strength begins to cross the Coulomb centre located at the origin of coordinates, which corresponds to nuclei collisions.

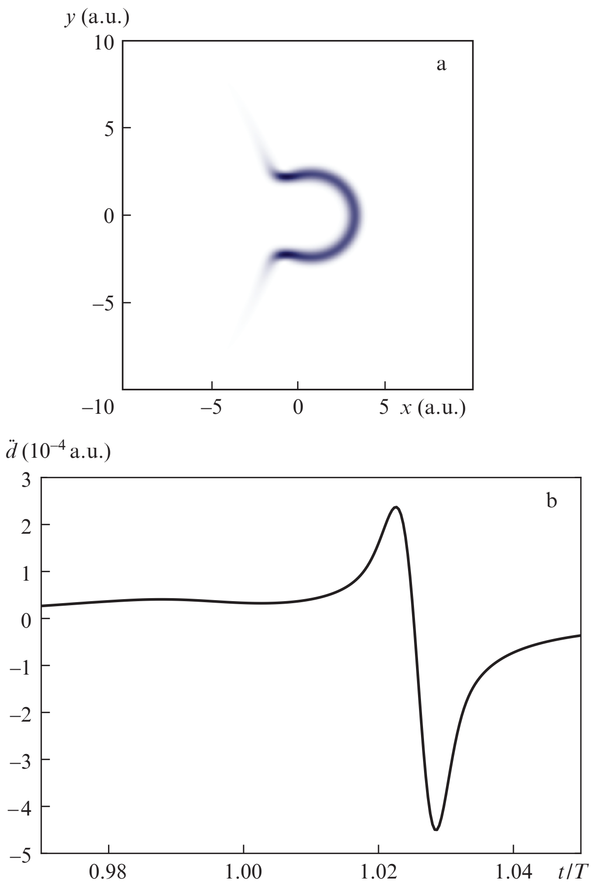

Figure 6. Results of two-dimensional quantum-mechanical calculations of the dynamics of nuclei of an HD molecule ionised by a laser field with intensity $I_0 = 3.3\times10^{19}$ W cm^{-2} and wavelength $\Lambda = 800$ nm: (a) probability density distribution over nuclear coordinates and (b) time dependence of dipole acceleration near the moment of collision of nuclei at $t \approx T$.

In the example presented in Fig. 6, the left side of the nuclear wave packet has this first intersection when it moves in the positive direction of the horizontal axis. As a result of the collision, the probability density distribution significantly changes near the intersection point with the Coulomb centre. In particular, there is a rupture of the original ring structure and there arise two outgoing probability density flows, symmetric about the horizontal axis, which correspond to the scattering of nuclei due to collisions. After changing the sign of the electric field, the horseshoe-shaped distribution formed in this way moves in the opposite direction, as can be seen from Fig. 6a, which shows the nuclear wave packet near the moment of intersection of the Coulomb centre. With the passage of this distribution through the Coulomb centre, only one strong polarisation burst appears (Fig. 6b) instead of two bursts arising in the one-dimensional case presented in Fig. 5 (the first burst in the two-dimensional case is almost completely suppressed due to the considered reason). Note that in an electric field with an increasing amplitude, each successive collision of nuclei occurs at a higher energy of $\mathcal{E}_{\rm coll}$, that is, the time of effective interaction of nuclei decreases, and, consequently, the changes in the nuclear wave function caused by these collisions gradually decrease.

Thus, below we will be interested in the characteristics of only the second burst, initiated by the right side of the nuclear wave packet, which does not change drastically due to the Coulomb interaction.

One can see from Fig. 5 that the duration of the second polarisation burst is about 13 as, and its intensity, which can be defined as $|\ddot{d}|^2$, is equal to $\sim1.9\times10^{-5}$ a.u. (which corresponds to a peak intensity of $\sim1.4\times10^5$ W cm^{-2} on the coherence length in a collimated beam; in the case of phase matching or quasi-phase-matching [32] and focusing of the harmonic radiation beam [33], this intensity can be several orders of magnitude greater). Figure 7a shows the spectrum, whose envelope indicates that photons with energies of the order of 100 eV are generated most efficiently, and the characteristic width of the spectrum is approximately 300 eV, while the spectrum extends up to energies of 600–700 eV. The resulting field burst is close to transform limited, since the corresponding product of the characteristic width of the spectrum and the pulse duration is of the order of unity. This also suggests that the mechanism under consideration makes it possible to obtain high-frequency radiation without attochirp. The latter is confirmed by the wavelet scalogram of the polarisation signal (details of the wavelet transform can be found elsewhere see [34]) shown in Fig. 7b, in which there are indeed no signs of attochirp.

Next, we consider how the characteristics (namely, the duration and intensity) of the polarisation burst change as functions of the laser radiation wavelength. Since in the approximation adopted by us the nuclear wave packet does not spread with time, the intensity of the resulting burst does not depend on the wavelength and, as indicated above, is equal to 1.9×10^{-5} a.u. As for the burst duration τ, it decreases with increasing wavelength (Fig. 8). In particular, at $I_0 = 3.3\times10^{19}$ W cm^{-2} and $\Lambda = 6400$ nm, it is equal to 2 as. This is explained by the fact that as the wavelength increases, the velocity of the wave packet increases proportionally, and since the nuclear wave packet does not spread, it passes through the Coulomb centre in less and less time.

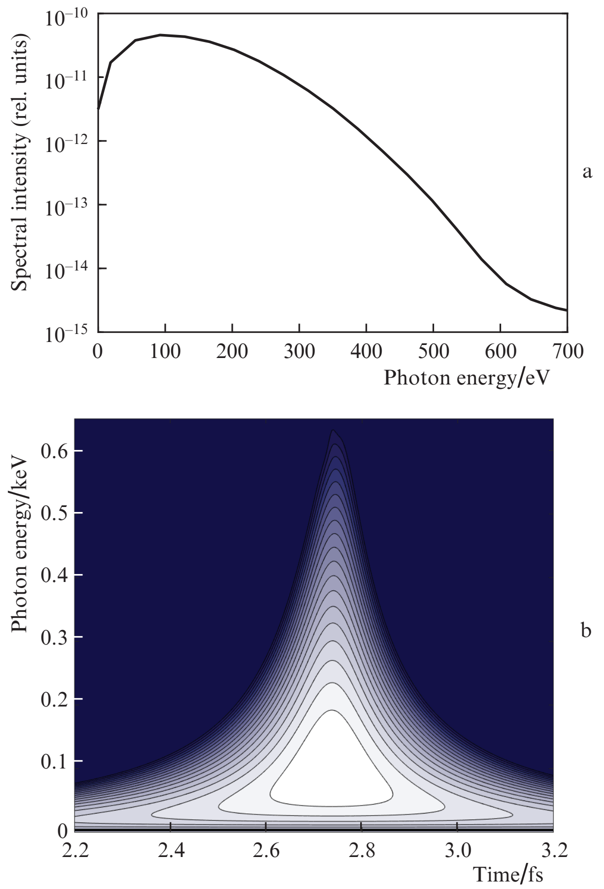

Figure 7. (a) Spectrum and (b) wavelet scalogram of the second dipole acceleration burst shown in Fig. 5.

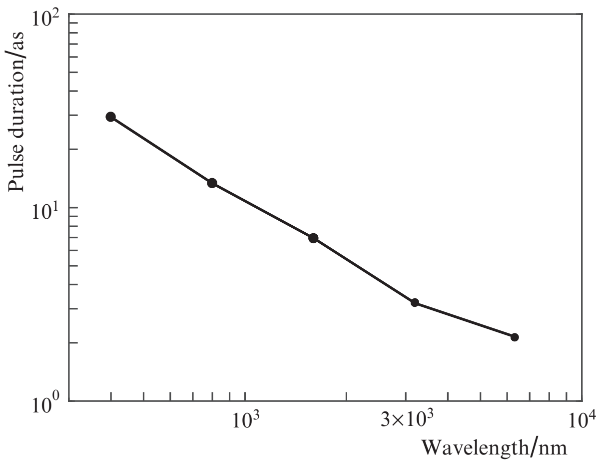

Figure 8. Classically calculated dependence of the dipole acceleration burst duration τ on the laser wavelength at $I_0 = 3.3\times10^{19}$ W cm^{-2} .

3. Quantum-mechanical calculations

Next, based on quantum-mechanical calculations, we consider the effect of the spreading of a nuclear wave packet on the characteristics of the generated attosecond burst. To this end, using the method of the split-step fast Fourier transform [35], we find the numerical solution of the nonstationary one-dimensional Schrödinger equation in the electric dipole approximation

$$\mathrm{i}\hbar\frac{\partial}{\partial t}\psi(x,t) = \left(-\frac{1}{2\mu}\frac{\partial^2}{\partial x^2} + \frac{\mathrm{i}q_{\mathrm{eff}}}{c\mu}A_x\frac{\partial}{\partial x} + \frac{qQ}{|x|}\right)\psi(x,t), \quad (11)$$

where

$$A_x = c\int_0^t E_0\exp(\gamma t)\sin(\Omega\tau)\,\mathrm{d}\tau$$

is the vector potential of the laser field. Using the Ehrenfest theorem, one can express the nonlinear part of the dipole acceleration (i.e., the polarisation response of two colliding nuclei) as

$$R(t) = -\int_{-\infty}^{\infty}\frac{\mathrm{d}V}{\mathrm{d}x}|\psi(x,t)|^2\,\mathrm{d}x, \quad (12)$$

where $V = qQ/|x|$ is the interaction potential of two nuclei.

Figure 9 shows the nuclear polarisation response for Λ = 3200 nm. One can seen that at the beginning of the first field period [at $t \approx (0.1-0.2)T$, where T is the field period), the left side of the nuclear wave packet experiences a collision at a low energy $\mathcal{E}_{\mathrm{coll}}$, which distorts its shape (the complex structure of the resulting burst is due to the reflection of part of the wave packet from the Coulomb centre). Then, the nuclear wave packet as a whole behaves like a classical particle, experiencing a collision leading to a series of polarisation bursts at $t \approx (0.92-1.02)T$ (see the inset in Fig. 9). As mentioned above, in the case of a more realistic multidimensional (even two-dimensional) consideration, the left side of the nuclear wave packet and the corresponding polarisation burst are strongly suppressed; therefore, as in Section 2, we will be interested only in the characteristics of the second dipole acceleration burst.

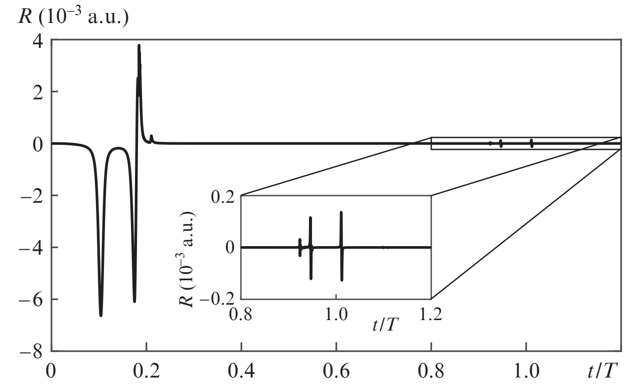

Figure 9. Time dependence of the polarisation response of the colliding nuclei, R, of the HD molecule, obtained as a result of a one-dimensional quantum-mechanical calculation at the laser intensity and wavelength of $I_0 = 3.3\times10^{19}$ W cm^{-2} and Λ = 3200 nm.

By approximating the right side of the nuclear wave packet at the initial time (Fig. 4) by a Gaussian curve with a characteristic width Δ_0 (in our case $\Delta_0 \approx 0.2$ a.u.), the width of the wave packet at the instant of collision, $t \approx T$, can be estimated as $\Delta(T) = \sqrt{\Delta_0^2 + \hbar^2T^2/(\Delta_0\mu)^2}$ [36]. It follows that in the case of the HD molecule, at $\Lambda > \mu c\Delta_0^2/\hbar \approx 350$ nm the second term in the expression for $\Delta(T)$ turns out to be larger than the first one. This means that at a laser wavelength exceeding 350 nm, the effect of spreading of the wave packet cannot be neglected.

It is seen from Fig. 10 that, as one would expect, the spreading of the nuclear wave packet leads to an increase in the duration of the burst being formed and to a decrease in its intensity (for example, at Λ = 800 nm, the intensity of the resulting pulse is approximately 5.6 times less than the pulse intensity found on the basis of classical calculations). Note that at wavelengths $\Lambda > 1600$ nm, the pulse duration tends to a constant value of approximately 22 as (Fig. 10a). This is due to the fact that at such wavelengths the width of the wave packet linearly increases with increasing Λ by the moment of collision. Because the relative velocity of the colliding nuclei also linearly increases with increasing wavelength, as can be seen from solution (6), the resulting burst duration does not depend on Λ. In addition, because the spreading of the wave packet leads to a decrease in the height of its peaks with time (cf. Figs 4 and 11) and, consequently, with increasing period T, the overlap integral (10) becomes smaller for longer wavelengths, which results in a decrease in the burst intensity (Fig. 10b).

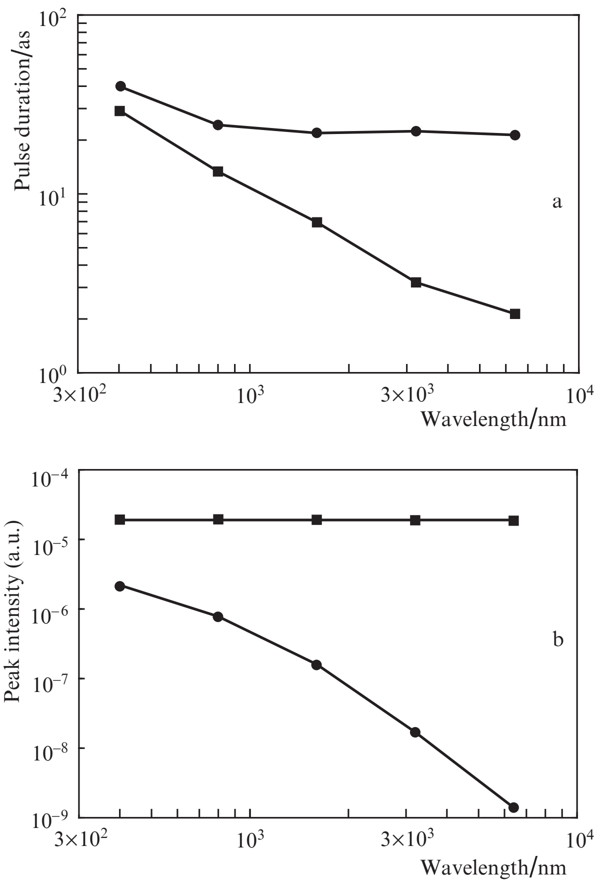

Figure 10. Dependence of (a) the duration and (b) peak intensity of the nonlinear polarisation response of the molecular system on the wavelength of the laser field at its intensity I_0 = 3.3×10^{19} W cm^{-2} . Squares and circles represent, respectively, the results of classical and quantum-mechanical calculations.

While for a given laser intensity the duration τ of the generated high-frequency burst is limited by the effect of the spreading of the nuclear wave packet, shorter bursts can be obtained by using more intense laser radiation. For example, for $I_0 = 3.3\times10^{21}$ W cm^{-2} and Λ = 800 nm, we get $\tau \approx 2.2$ as (Fig. 12).

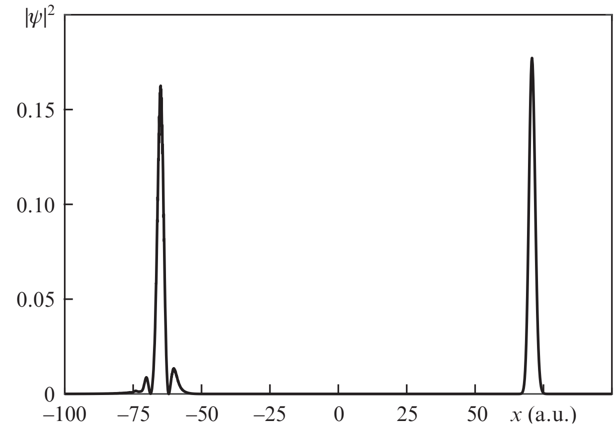

Figure 11. Probability density distribution over the nuclear coordinate at the time instant when $\langle x \rangle = 0$ at the laser intensity and wavelength of I_0 = 3.3×10^{19} W cm^{-2} and Λ = 3200 nm.

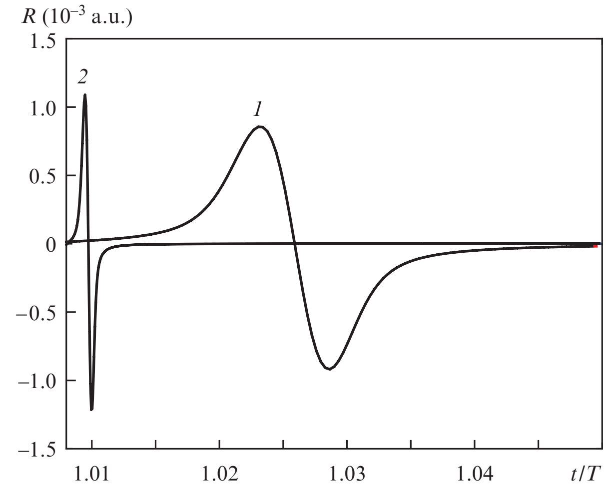

Figure 12. Time dependences of the polarisation response near the moment of collision of nuclei at the laser wavelength Λ = 800 nm and intensities I_0 = (*1*) 3.3×10^{19} and (*2*) 3.3×10^{21} W cm^{-2}.

4. Conclusions

This paper demonstrates the possibility of generating attosecond X-ray pulses without attochirp in Coulomb collisions of nuclei in an ensemble of diatomic molecules containing nuclei with different masses when they interact with ultraintense IR laser pulses. At a given intensity of radiation, the duration of the generated pulse as a function of the wavelength of the laser source is saturated at a certain level, determined by the spreading of the nuclear wave packet. With the radiation intensities available for modern petawatt laser systems, the pulse durations generated by laser-induced nuclear collisions can reach subattosecond values.

Acknowledgements. This work was supported by the Russian Foundation for Basic Research (Grant No. 18-02-00924) and the Presidium of the Russian Academy of Sciences (Fundamental Research Programme ‘Extreme Light Fields and Their Interaction with Matter’). Quantum-mechanical modelling was supported by the Russian Science Foundation (Grant No. 16-12-10279), the calculations in the framework of the classical model were supported by the Ministry of

Education and Science of the Russian Federation (Contract No. 14.W03.31.0032).

References

1. Corkum P.B., Krausz F. *Nat. Phys.*, **3**, 381 (2007).
2. Krausz F., Ivanov M. *Rev. Mod. Phys.*, **81**, 163 (2009).
3. Gallmann L., Cirelli C., Keller U. *Annu. Rev. Phys. Chem.*, **63**, 447 (2012).
4. Calegari F., Sansone G., Stagira S., Vozzi C., Nisoli M. *J. Phys. B: At. Mol. Opt. Phys.*, **49**, 062001 (2016).
5. Winterfeldt C., Spielmann C., Gerber G. *Rev. Mod. Phys.*, **80**, 117 (2008).
6. Kohler M.C., Pfeifer T., Hatsagortsyan K.Z., Keitel C.H. *Adv. At. Mol. Opt. Phys.*, **61**, 159 (2012).
7. Strelkov V.V., Platonenko V.T., Sterzhantov A.F., Ryabikin M.Yu. *Phys. Usp.*, **59**, 425 (2016) [*Usp. Fiz. Nauk*, **186**, 449 (2016)].
8. McPherson A., Gibson G., Jara H., Johann U., Luk T.S., McIntyre I.A., Boyer K., Rhodes C.K. *J. Opt. Soc. Am. B*, **4**, 595 (1987).
9. Ferray M., L'Huillier A., Li X.F., Lompré L.A., Mainfray G., Manus C. *J. Phys. B: At. Mol. Opt. Phys.*, **21**, L31 (1988).
10. Corkum P.B. *Phys. Rev. Lett.*, **71**, 1994 (1993).
11. Schafer K.J., Yang B., DiMauro L.F., Kulander K.C. *Phys. Rev. Lett.*, **70**, 1599 (1993).
12. Popmintchev T. et al. *Science*, **336**, 1287 (2012).
13. Zhao K., Zhang Q., Chini M., Wu Y., Wang X., Chang Z. *Opt. Lett.*, **37**, 3891 (2012).
14. Li J. et al. *Nat. Commun.*, **8**, 186 (2017).
15. Gaumnitz T., Jain A., Pertot Y., Huppert M., Jordan I., Ardana-Lamas F., Wörner H.J. *Opt. Express*, **25**, 27506 (2017).
16. Mairesse Y. et al. *Science*, **302**, 1540 (2003).
17. Kazamias S., Balcou Ph. *Phys. Rev. A*, **69**, 063416 (2004).
18. Kim K.T., Kim C.M., Baik M., Umesh G., Nam C.H. *Phys. Rev. A*, **69**, 051805(R) (2004).
19. López-Martens R. et al. *Phys. Rev. Lett.*, **94**, 033001 (2005).
20. Morlens A., Balcou P., Zeitoun P., Valentin C., Laude V., Kazamias S. *Opt. Lett.*, **30**, 1554 (2005).
21. Kim K.T., Kang K.S., Park M.N., Imran T., Umesh G., Nam C.H. *Phys. Rev. Lett.*, **99**, 223904 (2007).
22. Ko D.H., Kim K.T., Park J., Lee J.-H., Nam C.H. *New J. Phys.*, **12**, 063008 (2010).
23. Zheng Y., Zeng Z., Zou P., Zhang L., Li X., Liu P., Li R., Xu Z. *Phys. Rev. Lett.*, **103**, 043904 (2009).
24. Kohler M.C., Keitel C.H., Hatsagortsyan K.Z. *Opt. Express*, **19**, 4411 (2011).
25. Emelin M.Yu., Ryabikin M.Yu., Sergeev A.M., Chernobrovtseva M.D., Pfeifer T., Walter D., Gerber G. *Europhys. Lett.*, **69**, 913 (2005).
26. Sergeev A.M., Ryabikin M.Yu. *AIP Conf. Proc.*, **611**, 21 (2002).
27. Sokolov A.V., Zhi M. *J. Mod. Opt.*, **51**, 2607 (2004).
28. Zhi M., Sokolov A.V. *Phys. Rev. A*, **80**, 023415 (2009).
29. Lötstedt E., Midorikawa K. *Phys. Rev. Lett.*, **112**, 093001 (2014).
30. Smirnova O., Spanner M., Ivanov M. *Phys. Rev. Lett.*, **90**, 243001 (2003).
31. Kolos W., Wolniewicz L. *J. Chem. Phys.*, **43**, 2429 (1965).
32. Popmintchev T., Chen M.-C., Arpin P., Murnane M.M., Kapteyn H.C. *Nat. Photonics*, **4**, 822 (2010).
33. Mashiko H., Suda A., Midorikawa K. *Opt. Lett.*, **29**, 1927 (2004).
34. Emelin M.Yu., Ryabikin M.Yu., Sergeev A.M. *New J. Phys.*, **10**, 025026 (2008).
35. Fleck J.A. Jr, Morris J.R., Feit M.D. *Appl. Phys.*, **10**, 129 (1976).
36. Tannor D.J. *Introduction to Quantum Mechanics: A Time-Dependent Perspective* (Herndon, VA: University Science Books, 2007).